Quantifying the Gurken Morphogen Gradient in *Drosophila* Oogenesis

Lea A. Goentoro[1,4], **Gregory T. Reeves**[1], **Craig P. Kowal**[1,5], **Luigi Martinelli**[2], **Trudi Schüpbach**[3], and **Stanislav Y. Shvartsman**[1,*]

[1]Department of Chemical Engineering and Lewis-Sigler Institute for Integrative Genomics, Princeton University, Princeton, New Jersey 08544

[2]Department of Mechanical and Aerospace Engineering, Princeton University, Princeton, New Jersey 08544

[3]Howard Hughes Medical Institute and Department of Molecular Biology, Princeton University, Princeton, New Jersey 08544

Summary

Quantitative information about the distribution of morphogens is crucial for understanding their effects on cell-fate determination, yet it is difficult to obtain through direct measurements. We have developed a parameter estimation approach for quantifying the spatial distribution of Gurken, a TGFα-like EGFR ligand that acts as a morphogen in *Drosophila* oogenesis. Modeling of Gurken/EGFR system shows that the shape of the Gurken gradient is controlled by a single dimensionless parameter, the Thiele modulus, which reflects the relative importance of ligand diffusion and degradation. By combining the model with genetic alterations of EGFR levels, we have estimated the value of the Thiele modulus in the wild-type egg chamber. This provides a direct characterization of the shape of the Gurken gradient and demonstrates how parameter estimation techniques can be used to quantify morphogen gradients in development.

Introduction

Quantitative information about the spatial distribution of morphogens is essential for understanding how they induce cell fates in development (Gurdon and Bourillot, 2001; Martinez-Arias and Stewart, 2002). Molecular studies of development have discovered a large number of biochemical and cellular mechanisms that control the spatial range of diffusible ligands (Gonzalez-Gaitan, 2003; Tabata and Takei, 2004; Zhu and Scott, 2004). However, direct visualization of morphogen gradients is still in its early stages, largely due to the experimental difficulties associated with detecting extracellular diffusible molecules (Belenkaya et al., 2004; Kruse et al., 2004). A complete characterization of a morphogen

[*]Correspondence: stas@princeton.edu.
[4]Present address: Department of Systems Biology, Harvard Medical School, Boston, Massachusetts 02115.
[5]Present address: Division of Chemistry and Chemical Engineering, California Institute of Technology, Pasadena, California 91125.

gradient requires quantitative information about the concentration of a morphogen across the patterned field. To a first approximation, the shape of a morphogen gradient can be characterized by the ratio of the size of the patterned field (L) to the decay length of the patterning signal (λ). Clearly, this ratio must be regulated in any given patterning system. Indeed, when L/λ is small, the concentration of the inductive signal does not vary appreciably across the field, and all cells are exposed to the same signaling level. In the other extreme, the concentration decreases to its minimal value very quickly and most of the domain is again exposed to the same (but now low) level of signal. Based on this argument, one would expect that L can not be very different from λ for any morphogen gradient established by the combination of localized ligand secretion and uniform degradation. To test whether the prediction of this simple argument is true in a real system, we used a combination of modeling and experiments to estimate L/λ for a morphogen in *Drosophila* oogenesis.

The dorsoventral patterning in *Drosophila* oogenesis relies on the gradient of EGFR activation in the developing egg chamber (Nilson and Schupbach, 1999; Amiri and Stein, 2002). Gurken, one of the four ligands of *Drosophila* EGF receptor (Shilo, 2003), is secreted from the dorsal-anterior cortex of the oocyte and activates EGFR, which is uniformly expressed across the follicular epithelium (Schupbach, 1987; Neuman-Silberberg and Schupbach, 1994; Sapir et al., 1998; Ghiglione et al., 2002). The gradient of EGFR activation is established as a result of localized Gurken secretion, extracellular transport, binding to EGFR on the surface of the follicle cells, and receptor-mediated endocytic degradation (Roth, 2003). The current model of graded EGFR activation was deduced from clonal analyses experiments and studies of mutants with different levels of Gurken (Neuman-Silberberg and Schupbach, 1994; Roth and Schupbach, 1994; Pai et al., 2000; Ghiglione et al., 2002; James et al., 2002; Peri et al., 2002), but the gradient itself has not been visualized directly. Current visualization techniques detect only the Gurken molecules in the oocyte. Secreted Gurken is probably present at concentrations below the detection limits of current staining protocols. At the same time, attempts to express the GFP-tagged secreted Gurken in the oocyte have not been successful so far.

Genetic studies of EGFR signaling in *Drosophila* oogenesis and recent transcriptional profiling experiments suggest that Gurken controls the expression of tens to hundreds of genes in the follicular epithelium (Berg, 2005; Jordan et al., 2005). In order to accurately interpret the spatiotemporal responses to Gurken, quantitative information about the spatial distribution of secreted Gurken protein is required (Yakoby et al., 2005). Here, we report a parameter estimation strategy for quantifying the spatial distribution of the Gurken morphogen. Our approach relies on the combination of biophysical modeling, dimensional analysis, quantitative characterization of transcriptional response to Gurken in a number of genetic backgrounds, and on the quantitative assay for characterizing the Gal4/UAS targeted gene expression system (Goentoro et al., 2006). To our knowledge, the implementation of our parameter estimation approach provides the first characterization of the Gurken gradient and demonstrates how parameter estimation and genetic approaches can be productively combined to gain quantitative insights into the mechanisms of morphogenetic patterning.

Results

The Shape of the Gurken Gradient Depends on a Single Dimensionless Parameter

Given a full set of anatomical, cellular, and biochemical parameters, our model predicts the profile of secreted Gurken protein in the egg chamber (Figure 1C). Out of all model parameters, only the physical dimensions of the egg and the size of the source of Gurken secretion from the oocyte can be measured in a relatively straightforward way (Neuman-Silberberg and Schupbach, 1993; Spradling, 1993). Other parameters can be potentially measured, such as the binding constant of the Gurken/ EGFR interaction. This was previously done for Spitz, another ligand of *Drosophila* EGF receptor (Klein et al., 2004). The model also contains parameters, such as the effective extracellular diffusivity of Gurken, for which no direct experimental assays are currently available. Note however that, in order to characterize the shape of the Gurken gradient, it is not necessary to know every parameter in the original model. As shown in the Supplemental Data (available with this article online), the shape of the Gurken gradient is controlled by a single dimensionless number (Φ):

$$\Phi = \left(\frac{k_{on} k_e R}{(k_{off} + k_e)} \frac{L_{DV}^2}{DH \, sinh \, \xi_0} \right)^{0.5}, \quad (1)$$

where $\xi_o = \tanh^{-1} (L_{DV}/L_{AP})$, and all other parameters are defined in Figures 1A–1B. This number, known as the Thiele modulus in the engineering literature, can be related to the ratio of the geometric and dynamic length scales in the problem (Weisz, 1973; Bird et al., 2002; Saltzman, 2004; Griffith and Swartz, 2006). The geometric length scale is given by the linear dimension of the egg ($L \equiv L_{DV}$), while the dynamic length scale, defined as the distance on which the ligand concentration decays (λ), is given by $(DH(k_{off} + k_e)/k_{on} k_e R)^{0.5}$ (Pribyl et al., 2003; Berezhkovskii et al., 2004). Thus, $\Phi \sim L/\lambda$, with the proportionality constant related to the shape of the egg. The Gurken gradient computed for $\Phi = 1$ is shown in Figure 1C, where we have used L_{DV}/L_{AP} measured in wild-type egg chambers from stage 10A of oogenesis.

The Thiele modulus compares the relative importance of degradation and diffusion in the problem (Weisz, 1973; Bird et al., 2002). When transport dominates, which can be a consequence of either fast diffusion or slow degradation, the Thiele modulus is small, and the concentration field does not vary appreciably across the egg ($L \ll \lambda$). In the opposite regime, realized either by fast degradation or slow diffusion ($L \gg \lambda$), the decay distance is short, and the gradient is sharp. In this regime, Gurken molecules are captured and degraded in the very close proximity to the point of their release, and the shape of the Gurken gradient mirrors the spatial profile of its secretion from the oocyte.

The prediction of this simple argument is supported by the results of numerical analysis of the model (Figure 1D). We can use the ratio of concentrations of Gurken at the dorsalmost and the ventralmost points at the anterior boundary of the egg as the measure of the sharpness of the gradient. For shallow gradients, this ratio (g_V/g_D) will be close to unity, while for sharp gradients it will be close to zero. As expected, $g_V/g_D \approx 1$ when $\Phi \ll 1$, and $g_V/g_D \approx 0$ when $\Phi \gg 1$ (Figure 1D). Thus, based on the combination of the dimensional and

numerical analyses, we predict that "biologically useful" gradient (the one that is neither too shallow nor too sharp [Lander et al., 2002]) requires that the Thiele modulus is not very different from unity ($\Phi = O(1)$). Therefore, within the framework of our biophysical description, the problem of quantifying the Gurken gradient is reduced to the problem of estimating the Thiele modulus, the only free parameter in the model. Our strategy for estimating this parameter is based on the analysis of the transcriptional response to Gurken in genetic backgrounds with distinct levels of EGFR expression.

Using *pipe* as a Reporter Gene for Monitoring the Gurken Gradient

The *pipe* gene is an established transcriptional target of Gurken/EGFR signaling in the follicle cells (Sen et al., 1998). In the wild-type egg chamber, *pipe* is expressed in the ventral follicle cells (Figure 2A). Clonal analysis experiments with the EGFR pathway components established that *pipe* is directly repressed by Gurken-induced Ras/MAPK signaling (Pai et al., 2000; James et al., 2002; Peri et al., 2002). In combination with the sharp boundary of the *pipe* expression domain, this suggests a simple model in which *pipe* expression follows a switch-like dependence on the level of EGFR occupancy. In this model, the *pipe* expression is "on" when the EGFR occupancy is below some critical threshold C_T and "off" otherwise (Figure 2A). Therefore, within the framework of this model, the boundary of the *pipe* expression domain is the level set (i.e., the curve of constant concentration) on the surface of the follicular epithelium where the EGFR occupancy is equal to this critical threshold. This corresponds to the dimensionless Gurken concentration given by (see derivation in the Supplemental Data):

$$g(\eta^p, \theta^p) = \gamma \equiv C_T k_e / V, \quad (2)$$

where the dimensionless Gurken concentration is simply the Gurken concentration scaled by its maximal concentration in the absence of a gradient, i.e., $g(\eta, \theta) \equiv G(\eta, \theta)/G_0$; $G_0 \equiv k_{on} R k_e / (k_e + k_{off})$. The coordinates η and θ denote spatial location on the surface of the ellipsoid, which models the egg chamber (see Figure 1A and Figure S1A), and the superscript p indicates that the coordinates correspond to the pipe boundary. Each pair (η^p, θ^p) defines a point on the boundary of the pipe expression domain. Given a location of the boundary even at a single point in the follicular epithelium, one can determine the right-hand side of Equation 2 (γ) and in this way predict the two-dimensional boundary (η^p, θ^p). Figure 2B shows the predicted boundary, with γ derived from the location of the boundary of the wildtype pipe expression domain at the anteriormost section of the egg chamber.

As a solution of the model for the spatial distribution of the secreted Gurken, the left-hand side of Equation 2 depends on the value of the Thiele modulus (Φ), which is directly related to the multiple dimensional parameters of the biophysical model. In particular, according to Equation 1, Φ depends on the EGFR expression level in the follicle cells: $\Phi \sim R^{0.5}$. At the same time, the right hand side of Equation 2 (γ) does not depend on the EGFR expression level. Therefore, the boundary of the *pipe* expression domain must shift from its wild-type position in response to changes in the EGFR expression in the follicle cells (Figure 3A). Computational results confirm that the boundary of the *pipe* domain indeed shifts in response to under- and overexpression of EGFR (Figure 3B). Specifically, the *pipe*

expression domain expands upon EGFR overexpression and contracts upon decrease in the EGFR level. Qualitatively, this can be predicted from the results of the dimensional analysis. Indeed, higher levels of EGFR expression lead to a higher Thiele modulus (Equation 1), a sharper spatial profile of Gurken, and a readjustment of the *pipe* domain boundary (Figure 3B).

To validate this prediction of the model, we quantified the size of the *pipe* domain in egg chambers from late stage 9 to early stage 10B with different levels of EGFR expression in the follicular epithelium (Figure 4). We carefully selected the egg chambers in this time window given that the *pipe* expression remains constant during this stage of development. In addition, inspection of over 100 egg chambers per genotype confirmed that the *pipe* domain showed a smooth boundary without spatial bias. We measured the width of the *pipe* domain in wild-type egg chambers, in the egg chambers with a single copy of EGFR, and in the egg chambers in which EGFR was overexpressed by using the Gal4/UAS system. For the EGFR overexpression experiments, we used two drivers of different strengths (Gal4-E9 and Gal4-T155; for convenience, these drivers are called "weak" and "strong" in the rest of the text). In each of these genetic backgrounds, we measured the width of the *pipe* domain in anterior cross-sections at the precise position where the oocyte nucleus was visible. Our measurements show that the domain of *pipe* expression expands with increases in the receptor level and shrinks in the deficiency line (Figure 4). Using a linear regression model, we confirmed that the observed changes in the *pipe* domain are indeed statistically significant ($p < 0.001$). These results validate our biophysical model and set the stage for the quantitative characterization of the wild-type Gurken gradient.

Mathematical Framework for Parameter Estimation Approach

Our approach for estimating the wild-type value of the Thiele modulus is based on modeling the observed changes in the width of the *pipe* domain in response to EGFR overexpression. As shown in Figure 3B, depending on the starting value of the Thiele modulus, Φ_0, the domain of *pipe* exhibits differential sensitivity to changes in the receptor level. The higher the starting Thiele modulus, or the sharper the initial Gurken gradient, the more sensitive the domain of *pipe* is to changes in the receptor level. This is the basis for our parameter estimation procedure. By measuring the changes in the domain of *pipe* for a given level of perturbation in the EGFR level and fitting the measurements to the model, we can estimate the wild-type value of the Thiele modulus.

Let R_0, R_1, and R_2 be the levels of EGFR expression in the wild-type egg chamber and in the egg chambers in which EGFR is overexpressed by the weak and the strong Gal4 drivers, respectively. The fractional increase in receptor level driven by the weak driver is given by $f \equiv (R_1 - R_0)/R_0$, while the ratio of driver strengths, defined as the ratio of the excess receptors, is equal to $r \equiv (R_2 - R_0)/(R_1 - R_0)$. From Equation 1, the values of the Thiele moduli in genetic backgrounds with increased levels of EGFR are related to the wild-type value Φ_0: $\Phi_1 = \Phi_0(1 + f)^{0.5}$ and $\Phi_2 = \Phi_0(1 + fr)^{0.5}$. According to Equation 2, each value of Φ determines a corresponding boundary of the *pipe* expression domain.

Let $J(\theta, \Phi)$ denote the value of the dimensionless Gurken concentration (see the Supplemental Data for details) at the anterior boundary of the *pipe* expression domain,

measured in the egg chamber cross-sectioning experiment. As discussed in the previous section (see Equation 2), the dimensionless Gurken concentration at this boundary is not affected by changes in the EGFR expression level. Thus, $J(\theta, \Phi)$ is the same in all three genetic backgrounds. Denoting the locations of the anterior boundary of the *pipe* domain in the three backgrounds by θ_0, θ_1, and θ_2 and using the relations between the values of Φ in the three backgrounds, we arrive at the following system of equations:

$$J\left(\theta_1, \Phi_0(1+f)^{0.5}\right) - J(\theta_1, \Phi_0) = 0 \quad (3)$$

$$J\left(\theta_1, \Phi_0(1+f)^{0.5}\right) - J\left(\theta_2, \Phi_0(1+fr)^{0.5}\right) = 0. \quad (4)$$

These equations form the mathematical basis of our parameter estimation approach that provides a quantitative estimate of the wild-type Thiele modulus and, as a consequence, of the shape of the Gurken gradient. As described below, these equations are combined with the experimentally measured values of θ_0, θ_1, θ_2, and r and then solved for Φ_0 and f. Substitution of Φ_0 in the model equation reconstructs the wild-type Gurken gradient. Note that the terms in Equations 3 and 4 are not available explicitly but must be found numerically, by solving the boundary value problem for the steady-state Gurken concentration (see Equation M5 in the Supplemental Data).

Quantitative Estimation of the Thiele Modulus

The parameter estimation approach is implemented as follows. First, the median widths of *pipe* expression domain in wild-type and the two GAL4/UAS lines are used as estimates of θ_0, θ_1, and θ_2. Next, the ratio of the strengths of the strong and weak Gal4 drivers (r) is determined by using the GFP-based quantitative live imaging assay (Goentoro et al., 2006). We find that $r \approx 3 \pm 0.1$ for egg chambers from early stage 10A (see Supplemental Data for detailed measurement results). Finally, the egg aspect ratio is measured in egg chambers from early stage 10A. The egg chamber ratio $2L_{DV}/L_{AP}$ was found to be 0.76 ± 0.09; we have confirmed that it is not affected by changes in the receptor level (Table S1). Thus, there are five inputs to the parameter estimation procedure: the widths of the *pipe* domains in the three backgrounds, the relative strength of two Gal4 drivers, and the egg aspect ratio. This leaves Equations 3 and 4 with only two unknowns: f, the fractional increase of EGFR expression level by the weak driver, and Φ, the only dimensionless parameter in the biophysical model. The two equations are then solved numerically, by locating the global minimum of the sum of squares of the left hand sides of Equations 3 and 4. The confidence intervals for Φ and f are computed by Bootstrap approach, which involves resampling the measurement histograms of the *pipe* widths, the relative strength of the Gal4 drivers, and the egg aspect ratio (Efron and Tibshirani, 1993; Wasserman, 2003).

Following these steps, we find that the Thiele modulus in wild-type is 2.7, with the 90% confidence interval (1.5, 5.1) (see Figure 5F). Thus, our estimate suggests that the length scale of the signal is roughly one-third of the size of the patterned field. These numbers are fully consistent with our hypothesis that the ratio of the size of the patterned field to the

length scale of the patterning signal should be O(1) for all morphogens established by the combination of localized production and uniform degradation. Notice that the confidence intervals merely span 2-fold variations in either direction from the estimate. Using the estimate for $f \equiv (R_1 - R_0)/R_0$, we can compute the absolute level of receptor overexpression induced by the Gal4/UAS system at stage 10A. We find that the receptor protein level in Gal4-E9/UAS-EGFR and Gal4-T155/UAS-EGFR is ~1.8-fold and ~3.4-fold, respectively, of that in the wild-type. Using the estimated wild-type Thiele modulus to fit the measured *pipe* domain in the deficiency line, we find that the receptor protein level in the heterozygous deficiency line is ~60% of its wild-type level.

Using the estimated Thiele modulus, we can reconstruct the wild-type Gurken gradient (Figures 1E and 5D). In particular, we find that Gurken concentration at the ventral side is ~10% of that at the dorsal side. Thus, there is a nonzero Gurken concentration at the ventral side, in agreement with the proposed role of Gurken as a long-ranged secreted signal in patterning of the follicular epithelium (Pai et al., 2000). It is also possible to compute the relative Gurken concentration corresponding to the boundaries of high- and low-threshold targets of Gurken/EGFR signaling. Gurken signaling induces expression of *kekkon* and sprouty in roughly one-third of the dorsal region (Ghiglione et al., 1999; Peri et al., 1999). Based on the estimated Thiele modulus, the Gurken concentration at the *pipe* boundary is ~30% of its value at the *kekkon/sprouty* boundary. Thus, the two threshold responses in Gurken-EGFR signaling are established by a mere 3-fold difference in Gurken concentration.

Discussion

Like many other morphogens, the spatial distribution of secreted Gurken protein in *Drosophila* oogenesis cannot be visualized directly at this time. Here, we have demonstrated that the shape of the Gurken morphogen can be characterized with a combination of modeling and experimental approaches. Our approach yields not only a qualitative depiction of the Gurken gradient but also a quantitative understanding on how the Gurken gradient is regulated and responds to perturbations. We have formulated a biophysical model for Gurken extracellular transport and receptor-mediated degradation. Through the dimensional analysis of the model, we have established that the shape of the spatial distribution of active Gurken protein is controlled by just a single dimensionless number, which combines multiple tissue, cellular, and molecular parameters. We have then developed and implemented a model-based approach for estimating the value of this dimensionless number from experiments involving variations in EGFR expression levels. The estimated Gurken gradient is fully consistent with its role as a long-range patterning signal in *Drosophila* oogenesis (Amiri and Stein, 2002; Roth, 2003). This demonstrates how model-based parameter estimation can be combined with genetic experiments and quantitative measurements to derive a systemslevel property of a patterning signal. From the standpoint of the analysis of *Drosophila* oogenesis, quantitative characterization of the Gurken gradient enables more detailed models of pattern formation initiated by this morphogen. For example, it is now possible to quantify the distinct thresholds in the Gurken signal which define boundaries of the expression of a large number of Gurken targets in the follicular epithelium (Jordan et al., 2005; Yakoby et al., 2005).

While modeling of developmental processes is not new (Eldar et al., 2002; Shvartsman et al., 2002; Kruse et al., 2004; Mizutani et al., 2005; Shimmi et al., 2005), model-based reconstruction of concentration profiles in patterning systems has been done only in one experimental system (Jaeger et al., 2004). Reinitz and colleagues used modeling, imaging, and optimization approaches to reconstruct the regulatory interactions in the AP patterning of the *Drosophila* embryo. Parameter estimation was based on the dynamic data in the wildtype embryo, and the generated estimates of parameters were not unique (the estimates themselves were generated by a stochastic optimization approach). In our work, parameter estimation is done at steady state and relies on data from both wild-type and mutant genotypes. Furthermore, deterministic parameter estimation allows us to both claim that the resulting parameter estimate is unique and carry out detailed error analysis.

We have estimated the wild-type value of the dimensionless group that controls the sharpness of the Gurken gradient. As a result, we find that the gradient operates in the regime where EGFR not only transduces the Gurken signal, but also regulates its spatial range across the follicular epithelium. The possibility for the regulation of the spatial range of a diffusible signal by the level of the cognate cell surface receptor was first recognized in the Torso signaling pathway in the *Drosophila* embryo (Casanova and Struhl, 1993) and, since then, has been identified in a number of patterning contexts (Lecuit and Cohen, 1998; Teleman et al., 2001). Our results, based on the EGFR-deficiency line and two EGFR overexpression experiments, demonstrate that such a "ligand trapping" effect is also operative in *Drosophila* oogenesis. In addition, our biophysical modeling shows how the spatial range of the Gurken signal is dictated by the relative influence of the various processes in the system.

The sensitivity of the Gurken gradient (and *pipe* domain) to EGFR expression levels observed in our experiments is not at odds with the established robustness of the embryonic dorsoventral patterning. Previous work has shown that downstream processes can successfully buffer significant variations in the width of *pipe* expression domain (Nilson and Schupbach, 1998; Peri et al., 2002). Our model predicts a further increase in the width of the *pipe* domain for even stronger levels of EGFR overexpression. We have used a number of strong Gal4 drivers to test this experimentally and discovered that, contrary to the prediction, the *pipe* domain starts to contract above certain level of EGFR over-expression (results not shown). Specifically, we used Gal4-GR1 (GR1/E9 ~9-fold) and Gal4-CY2 (CY2/E9 ~14-fold), where the relative strengths were measured with UAS-EGFR-EGFP at stage 10A. This observation can be explained by ligand-independent EGFR activation (Schweitzer et al., 1995), an effect not included in our model, and the presence of Spitz-positive feedback at the dorsal region. While our model can be extended to include a more detailed description of receptor activation, trafficking dynamics, and the subsequent feedback loops, we believe that the presented model is adequate for the parameter estimation purpose of this paper.

Our parameter estimation approach provides the first estimate for the sharpness of the Gurken gradient, defined as the ratio of the size of the field patterned by Gurken (L) and the decay length of the Gurken signal (λ). The fact that this ratio was determined to be of order one ($L/\lambda \sim 2.7$) supports the dimensional argument that suggests that L can not be very

different from λ in all patterning systems where the morphogen gradient is established through the combination of localized production and uniform degradation. This hypothesis is further supported by the recent demonstration of the fact that, for the Bicoid gradient, the value of L/λ is conserved in three different fly species (Gregor et al., 2005). In the future, it will be important to determine L/λ for other morphogens and to extend our approach to systems where the spatial distribution of morphogens is controlled by feedback loops (Freeman, 2000; Eldar et al., 2003; Reeves et al., 2005).

Over the past two decades *Drosophila* oogenesis has emerged as one of the most extensively studied models of epithelial pattern formation (Dobens and Raftery, 2000; Berg, 2005; Yakoby et al., 2005). Until recently, all of the mechanisms in this system were derived on the basis of genetic experiments, and their quantitative analysis has been limited by the inability to directly examine the patterning inputs (Neuman-Silberberg and Schupbach, 1994; Wasserman and Freeman, 1998). Our description of the Gurken gradient provides the first step toward the quantitative model of pattern formation in the follicular epithelium and will allow an assessment of the threshold of gene expression for target genes of the Egf receptor (Figure 6). In the future, our analysis coupled with the precise analysis of transcriptional responses to Gurken (Morimoto et al., 1996; Dobens et al., 2000; Atkey et al., 2006) and its interaction with other signaling pathways (Peri and Roth, 2000; Dobens et al., 2005; Ward et al., 2006) should lead to a comprehensive, quantitative description of patterning in this tissue.

Experimental Procedures

Biophysical Model of Gurken Transport and Degradation

The dimensions of the egg chamber and model geometry are defined in Figure 1A. The key processes in the model are shown in Figure 1B. We model Gurken secretion from the oocyte, extracellular transport with effective diffusivity D, reversible binding to EGFR (with rate constants k_{on} and k_{off}), and receptor-mediated endocytosis (with rate constant k_e; Wiley and Cunningham, 1981). V is the constant flux of ligand from the dorsal-anterior cortex of the oocyte. The size of the Gurken source is approximated from published images of Gurken protein (Neuman-Silberberg and Schupbach, 1996; Norvell et al., 1999; Queenan et al., 1999). Previous studies of the Gurken/EGFR signaling in oogenesis suggest that patterning of the follicular epithelium proceeds in the ligand-limited regime (Neuman-Silberberg and Schupbach, 1994; Peri et al., 2002) and that the level and the spatial pattern of EGFR expression is constant during the time window considered in this work (Sapir et al., 1998). Thus, we assume that the level of EGFR expression is constant; the cell-surface density of EGFR in the follicle cells is denoted by R. In addition, order-of-magnitude estimates of the rates of Gurken transport, binding, and degradation suggest that the spatial distribution of Gurken corresponds to the steady state of the model. Assuming that ligand concentration does not vary across the gap between the oocyte and the follicle cells, and nondimensionalizing the steady-state problem, one can show that the shape of the Gurken gradient depends on a single dimensionless parameter, which compares the relative strengths of ligand degradation and diffusion. See the Supplemental Data for the details of the model, dimensional analysis, and numerical methods.

Genetic Manipulation of EGFR Levels in the Follicle Cells

To decrease the EGFR expression level, we used the heterozygous deficiency *Drosophila* line, Df(2R)top[c18a]/+, which carries only one copy of the EGFR gene (Price et al., 1989). To increase the receptor level, we used the Gal4/UAS targeted expression system (Brand and Perrimon, 1993). We used the UAS-EGFR as the responder line (Buff et al., 1998). To find the appropriate Gal4 drivers, we performed a quantitative analysis of ~15 Gal4 drivers, which allowed us to rank various drivers based on their strength of expression. The details of the GFP-based assay used for quantifying the relative strengths of Gal4 drivers were reported elsewhere (Goentoro et al., 2006). Two relatively weak Gal4 drivers were selected from the screen: Gal4-T155 (Brand and Perrimon, 1994) and the weaker Gal4-E9. The spatial profiles of Gal4-E9 and Gal4-T155 are shown in Figure S2 of the Supplemental Data. We observed a spatially variegated expression in all Gal4 drivers examined. With respect to Gal4-E9 and Gal4-T155, the pattern of Gal4 expression is patchy, but random, i.e., with no obvious pattern across the AP- or DV-axis. For every driver, we have examined over 100 eggs and observed no spatial bias. Despite the patchy pattern of receptor overexpression, the resulting domain of *pipe* is uniform, and the boundary of *pipe* expression is smooth. The temporal profiles of the Gal4 drivers were analyzed with UAS-EGFP (Halfon et al., 2002) and UAS-EGFR-EGFP (a gift from J. Duffy) as the reporter proteins. EGFP fluorescence was detected as early as in stage 7/8 in Gal4-E9 and stage 2/3 in Gal4-T155. Thus, both drivers are active during the stages relevant for this study (i.e., stages 9–10B).

Quantifying the Relative Strengths of Genetic Perturbations

To quantify the relative strength of Gal4-T155 and Gal4-E9 (T155/E9) expression, we used the quantitative fluorescence assay (Goentoro et al., 2006). Since the Gal4 expression varies over time, we focused our measurements on a relatively narrow small time window, the early stage 10A, which can be identified by the follicle cell morphology (Spradling, 1993), see below. The ease in identifying the time period is necessary to ensure consistency across experiments. Egg chambers from four genotypes were examined: Gal4-T155/UAS-EGFR-EGFP, Gal4-E9/UAS-EGFR-EGFP, Gal4-T155/UAS-EGFP, and Gal4-E9/UAS-EGFP. Each genotype was imaged in 3 independent measurements of 10 to 15 egg chambers from early stage 10A. We found similar T155/E9 ratios from imaging analysis with UAS-EGFR-EGFP and UAS-EGFP, even though the two reporter proteins exhibit large difference in their stability. This indicates that the measured T155/E9 ratio is not dependent on the reporter protein used and is therefore applicable when the two Gal4 drivers are used to activate UAS-EGFR. We conclude that the T155/E9 ratio quantified with UAS-EGFR-EGFP responder is a good estimate of the relative amount of extra receptors in Gal4-T155/UAS-EGFR and Gal4-E9/UAS-EGFR, see also (Goentoro et al., 2006). We did not use the UAS-EGFR-EGFP construct in the measurements of the *pipe* expression domain since our results (data not shown) strongly suggest that the signaling potency of the UAS-EGFR-EGFP construct is stronger than that of the UAS-EGFR construct. Thus, we have chosen to work with the UAS-EGFR lines for our experiments.

In Situ Hybridization and Measurements of the *pipe* Expression Domain

The domain of *pipe* expression was visualized by in situ hybridization. The digoxigenin-labeled *pipeST2* RNA probe (Pai et al., 2000) was prepared with the DIG RNA Labeling Kit (Boehringer Mannheim). Fly stocks and crosses were maintained at room temperature. Flies were placed on yeast for 2 days before dissection, at room temperature. Ovaries were dissected in cold PBS, partially separated, and fixed in 4% paraformaldehyde in PBS, 10% DMSO, and heptane for 20 min. In situ hybridization was performed according to (Tautz and Pfeifle, 1989) with some modifications (Suter and Steward, 1991; Kosman et al., 2004). Stained egg chambers were cross-sectioned around the oocyte-nurse cell boundary with 26G1/2 hypodermic needles (Becton Dickinson & Co.), as described in (Dawes-Hoang et al., 2005). The cross-sections were imaged with a Nikon E800 microscope. The 40× Nomarski images of the cross-sections were collected from the focal plane where the oocyte nucleus is visible. The width of the *pipe* expression domain was measured at this focal plane. Image analysis was performed with the IP Lab software. The measurements were collected from egg chambers between late stage 9 and early stage 10B, during which *pipe* expression is known to be constant.

Measurements of Egg Dimensions

Egg dimensions were measured from their Nomarski images. In particular, from each egg chamber, we measured the anterior circumference of the oocyte and the aspect ratio of the oocyte. Fixed egg chambers were separated by hand and placed on a grid drawn on a glass slide, immersed in PBS buffer. The egg chambers were imaged individually using a 20× magnification in a Nikon E800 microscope (without a cover slip). From the image, the stages were assigned, and the aspect ratio for each egg chamber was measured. Each egg chamber was subsequently cross-sectioned and placed in the same position within the grid, immersed in Aquapolymount. The cross-sections were then imaged with a 40× magnification at the focal plane where the oocyte nucleus was visible. The egg diameter was measured from the cross-section images. Using the measurement protocol described above, we confirmed that there are no significant differences ($p < 0.05$) in the egg dimensions from wt, Gal4-T155/UAS-EGFR, and Gal4-E9/UAS-EGFR.

Combining Modeling and Measurements

The steady-state solution of the model is valid from late stage 9 to stage 10B, as evidenced by the constant domain of *pipe* expression. The measurements of the *pipe* domains were performed on egg chambers from late stage 9 to early stage 10B, during which the domain of *pipe* expression remains at a constant proportion of the egg chamber. The measurements of the *pipe* domains are therefore applicable for any smaller time window within the period where the measurements were collected. The measurements of the T155/E9 ratio were performed on egg chambers from early stage 10A, as described above. Accordingly, measurements of the egg dimensions were performed on egg chambers from early stage 10A. We define the early stage 10A as the period where the follicle cells have just finished their posterior migration, such that the anterior boundary of the follicular epithelium is still at an angle with the oocyte. The presented estimate of the Thiele modulus of the Gurken gradient is therefore valid for wild-type egg chambers from early stage 10A.

Supplementary Material

Refer to Web version on PubMed Central for supplementary material.

Acknowledgments

References

Amiri A, Stein D. Dorsoventral patterning: a direct route from ovary to embryo. Curr Biol. 2002; 12:R532–R534. [PubMed: 12176378]

Atkey MR, Lachance JF, Walczak M, Rebello T, Nilson LA. Capicua regulates follicle cell fate in the *Drosophila* ovary through repression of mirror. Development. 2006; 133:2115–2123. [PubMed: 16672346]

Belenkaya TY, Han C, Yan D, Opoka RJ, Khodoun M, Liu H, Lin X. *Drosophila* Dpp morphogen movement is independent of dynamin-mediated endocytosis but regulated by the glypican members of heparan sulfate proteoglycans. Cell. 2004; 119:231–244. [PubMed: 15479640]

Berezhkovskii AM, Batsilas L, Shvartsman SY. Ligand trapping in epithelial layers and cell cultures. Biophys Chem. 2004; 107:221–227. [PubMed: 14967237]

Berg CA. The *Drosophila* shell game: patterning genes and morphological change. Trends Genet. 2005; 21:346–355. [PubMed: 15922834]

Bird, RB.; Stewart, WE.; Lightfoot, EN. Transport Phenomena. Second Edition. New York: John Wiley & Sons; 2002.

Brand AH, Perrimon N. Targeted gene expression as a means of altering cell fates and generating dominant phenotypes. Development. 1993; 118:401–415. [PubMed: 8223268]

Brand AH, Perrimon N. Raf acts downstream of the EGF receptor to determine dorsoventral polarity during *Drosophila* oogenesis. Genes Dev. 1994; 8:629–639. [PubMed: 7926754]

Buff E, Carmena A, Gisselbrecht S, Jimenez F, Michelson A. Signalling by the *Drosophila* epidermal growth factor receptor is required for the specification and diversification of embryonic muscle progenitors. Development. 1998; 125:2075–2086. [PubMed: 9570772]

Casanova J, Struhl G. The torso receptor localizes as well as transduces the spatial signal specifying terminal body pattern in *Drosophila*. Nature. 1993; 362:152–155. [PubMed: 8450886]

Dawes-Hoang RE, Parmar KM, Christiansen AE, Phelps CB, Brand AH, Wieschaus EF. *folded gastrulation*, cell shape change and the control of myosin localization. Development. 2005; 132:4165–4178. [PubMed: 16123312]

Dobens LL, Raftery LA. Integration of epithelial patterning and morphogenesis in *Drosophila* oogenesis. Dev Dyn. 2000; 218:80–93. [PubMed: 10822261]

Dobens LL, Peterson JS, Treisman J, Raftery LA. *Drosophila* bunched integrates opposing DPP and EGF signals to set the operculum boundary. Development. 2000; 127:745–754. [PubMed: 10648233]

Dobens L, Jaeger A, Peterson JS, Raftery LA. Bunched sets a boundary for Notch signaling to pattern anterior eggshell structures during *Drosophila* oogenesis. Dev Biol. 2005; 287:425–437. [PubMed: 16223477]

Efron, B.; Tibshirani, RJ. An Introduction to the Bootstrap. Boca Raton, FL: Chapman & Hall/CRC; 1993.

Eldar A, Dorfman R, Weiss D, Ashe H, Shilo BZ, Barkai N. Robustness of the BMP morphogen gradient in *Drosophila* embryonic patterning. Nature. 2002; 419:304–308. [PubMed: 12239569]

Eldar A, Rosin D, Shilo BZ, Barkai N. Self-enhanced ligand degradation underlies robustness of morphogen gradients. Dev Cell. 2003; 5:635–646. [PubMed: 14536064]

Freeman M. Feedback control of intercellular signalling in development. Nature. 2000; 408:313–319. [PubMed: 11099031]

Ghiglione C, Carraway KL, Amundadottir LT, Boswell RE, Perrimon N, Duffy JB. The transmembrane molecule kekkon 1 acts in a feedback loop to negatively regulate the activity of the *Drosophila* EGF receptor during oogenesis. Cell. 1999; 96:847–856. [PubMed: 10102272]

Ghiglione C, Bach EA, Paraiso Y, Carraway KL, Noselli S, Perrimon N. Mechanism of activation of the *Drosophila* EGF Receptor by the TGFalpha ligand Gurken during oogenesis. Development. 2002; 129:175–186. [PubMed: 11782411]

Goentoro LA, Yakoby N, Goodhouse J, Schupbach T, Shvartsman SY. Quantitative analysis of the GAL4/UAS system in *Drosophila* oogenesis. Genesis. 2006; 44:66–74. [PubMed: 16425298]

Gonzalez-Gaitan M. Signal dispersal and transduction through the endocytic pathway. Nat Rev Mol Cell Biol. 2003; 3:213–224. [PubMed: 12612640]

Gregor T, Bialek W, de Ruyter van Steveninck RR, Tank DW, Wieschaus EF. Diffusion and scaling during early embryonic pattern formation. Proc Natl Acad Sci USA. 2005; 102:18403–18407. [PubMed: 16352710]

Griffith LG, Swartz MA. Capturing complex 3D tissue physiology in vitro. Nat Rev Mol Cell Biol. 2006; 7:211–224. [PubMed: 16496023]

Gurdon JB, Bourillot PY. Morphogen gradient interpretation. Nature. 2001; 413:797–803. [PubMed: 11677596]

Halfon MS, Gisselbrecht S, Lu J, Estrada B, Keshishian H, Michelson AM. New fluorescent protein reporters for use with the *Drosophila* Gal4 expression system and for vital detection of balancer chromosomes. Genesis. 2002; 34:135–138. [PubMed: 12324968]

Jaeger J, Surkova S, Blagov M, Janssens H, Kosman D, Kozlov KN, Manu Myasnikova E, Vanario-Alonso CE, Samsonova M, et al. Dynamic control of positional information in the early *Drosophila* embryo. Nature. 2004; 430:368–371. [PubMed: 15254541]

James KE, Dorman JB, Berg CA. Mosaic analyses reveal the function of *Drosophila* Ras in embryonic dorsoventral patterning and dorsal follicle cell morphogenesis. Development. 2002; 129:2209–2222. [PubMed: 11959829]

Jordan KC, Hatfield SD, Tworoger M, Ward EJ, Fischer KA, Bowers S, Ruohola-Baker H. Genome wide analysis of transcript levels after perturbation of the EGFR pathway in the *Drosophila* ovary. Dev Dyn. 2005; 232:709–724. [PubMed: 15704171]

Klein D, Nappi VM, Reeves GT, Shvartsman SY, Lemmon MA. Argos inhibits epidermal growth factor receptor signalling by ligand sequestration. Nature. 2004; 430:1040–1044. [PubMed: 15329724]

Kosman D, Mizutani CM, Lemons D, Cox WG, McGinnis W, Bier E. Multiplex detection of RNA expression in *Drosophila* embryos. Science. 2004; 305:846. [PubMed: 15297669]

Kruse K, Pantazis P, Bollenbach T, Julicher F, Gonzalez-Gaitan M. Dpp gradient formation by dynamin-dependent endocytosis: receptor trafficking and the diffusion model. Development. 2004; 131:4843–4856. [PubMed: 15358671]

Lander AD, Nie W, Wan FY. Do morphogen gradients arise by diffusion? Dev Cell. 2002; 2:785–796. [PubMed: 12062090]

Lecuit T, Cohen SM. Dpp receptor levels contribute to shaping the Dpp morphogen gradient in the *Drosophila* wing imaginal disc. Development. 1998; 125:4901–4907. [PubMed: 9811574]

Martinez-Arias, A.; Stewart, A. Molecular Principles of Animal Development. New York, NY: Oxford University Press; 2002.

Mizutani CM, Nie Q, Wan FY, Zhang YT, Vilmos P, Sousa-Neves R, Bier E, Marsh JL, Lander AD. Formation of the BMP activity gradient in the *Drosophila* embryo. Dev Cell. 2005; 8:915–924. [PubMed: 15935780]

Morimoto AM, Jordan KC, Tietze K, Britton JS, O'Neill EM, Ruohola-Baker H. Pointed, an ETS domain transcription factor, negatively regulates the EGF receptor pathway in *Drosophila* oogenesis. Development. 1996; 122:3745–3754. [PubMed: 9012496]

Neuman-Silberberg FS, Schupbach T. The *Drosophila* dorsoventral patterning gene gurken produces a dorsally localized RNA and encodes a TGF alpha-like protein. Cell. 1993; 75:165–174. [PubMed: 7691414]

Neuman-Silberberg FS, Schupbach T. Dorsoventral axis formation in *Drosophila* depends on the correct dosage of the gene gurken. Development. 1994; 120:2457–2463. [PubMed: 7956825]

Neuman-Silberberg FS, Schupbach T. The *Drosophila* TGF-alpha-like protein: expression and cellular localization during *Drosophila* oogenesis. Mech Dev. 1996; 59:105–113. [PubMed: 8951789]

Nilson LA, Schupbach T. Localized requirements for *windbeutel* and *pipe* reveal a dorsoventral prepattern within the follicular epithelium of the *Drosophila* ovary. Cell. 1998; 93:253–262. [PubMed: 9568717]

Nilson LA, Schupbach T. EGF receptor signaling in *Drosophila* oogenesis. Curr Top Dev Biol. 1999; 44:203–243. [PubMed: 9891881]

Norvell A, Kelley RL, Wehr K, Schupbach T. Specific isoforms of Squid, a *Drosophila* hnRNP, perform distinct roles in Gurken localization during oogenesis. Genes Dev. 1999; 13:864–876. [PubMed: 10197986]

Pai L, Barcelo G, Schupbach T. D-cbl, negative regulator of the Egfr pathway, is required for dorsoventral patterning in *Drosophila* oogenesis. Cell. 2000; 103:51–61. [PubMed: 11051547]

Peri F, Roth S. Combined activities of Gurken and Decapentaplegic specify dorsal chorion structures of the *Drosophila* egg. Development. 2000; 127:841–850. [PubMed: 10648242]

Peri F, Bokel C, Roth S. Local Gurken signaling and dynamic MAPK activation during *Drosophila* oogenesis. Mech Dev. 1999; 81:75–88. [PubMed: 10330486]

Peri F, Technau M, Roth S. Mechanisms of Gurken-dependent *pipe* regulation and the robustness of dorsoventral patterning in *Drosophila*. Development. 2002; 129:2965–2975. [PubMed: 12050143]

Pribyl M, Muratov CB, Shvartsman SY. Discrete models of autocrine signaling in epithelial layers. Biophys J. 2003; 84:3624–3635. [PubMed: 12770871]

Price JV, Clifford RJ, Schupbach T. The maternal ventralizing locus torpedo is allelic to faint little ball, an embryonic lethal, and encodes the *Drosophila* EGF receptor homolog. Cell. 1989; 56:1085–1092. [PubMed: 2493993]

Queenan AM, Barcelo G, VanBuskirk C, Schupbach T. The transmembrane region of Gurken is not required for biological activity, but is necessary for transport to the oocyte membrane in *Drosophila*. Mech Dev. 1999; 89:35–42. [PubMed: 10559478]

Reeves GT, Kalifa R, Klein D, Lemmon MA, Shvartsman SY. Computational analysis of EGFR inhibition by Argos. Dev Biol. 2005; 284:523–535. [PubMed: 15982648]

Roth S. The origin of dorsoventral polarity in *Drosophila*. Philos Trans R Soc Lond B Biol Sci. 2003; 358:1317–1329. [PubMed: 14511478]

Roth S, Schupbach T. The relationship between ovarian and embryonic dorsoventral patterning in *Drosophila*. Development. 1994; 120:2245–2257. [PubMed: 7925025]

Saltzman, WM. Tissue Engineering: Engineering Principles for the Design of Replacement Organs and Tissues. Oxford, UK: Oxford University Press; 2004.

Sapir A, Schweitzer R, Shilo BZ. Sequential activation of the EGF receptor pathway during *Drosophila* oogenesis establishes the dorsoventral axis. Development. 1998; 125:191–200. [PubMed: 9486793]

Schupbach T. Germ line and soma cooperate during oogenesis to establish the dorsoventral pattern of the egg shell and embryo in *Drosophila melanogaster*. Cell. 1987; 49:699–707. [PubMed: 3107840]

Schweitzer R, Shaharabany M, Seger R, Shilo BZ. Secreted Spitz triggers the DER signaling pathway and is a limiting component in embryonic ventral ectoderm determination. Genes Dev. 1995; 9:1518–1529. [PubMed: 7601354]

Sen J, Goltz JS, Stevens L, Stein D. Spatially restricted expression of *pipe* in the *Drosophila* egg chamber defines embryonic dorsal-ventral polarity. Cell. 1998; 95:471–481. [PubMed: 9827800]

Shilo BZ. Signaling by the *Drosophila* epidermal growth factor receptor pathway during development. Exp Cell Res. 2003; 284:140–149. [PubMed: 12648473]

Shimmi O, Umulis D, Othmer H, O'Connor MB. Facilitated transport of a Dpp/Scw heterodimer by Sog/Tsg leads to robust patterning of the *Drosophila* blastoderm embryo. Cell. 2005; 120:873–886. [PubMed: 15797386]

Shvartsman SY, Muratov CB, Lauffenburger DA. Modeling and computational analysis of EGF receptor-mediated cell communication in *Drosophila* oogenesis. Development. 2002; 129:2577–2589. [PubMed: 12015287]

Spradling, AC. Developmental genetics of oogenesis. In: Bate, M.; Arias, AM., editors. The Development of *Drosophila melanogaster*. Plainview, NY: Cold Spring Harbor Laboratory Press; 1993. p. 1-70.

Suter B, Steward R. Requirement for phosphorylation and localization of the Bicaudal-D protein in *Drosophila* oocyte differentiation. Cell. 1991; 67:917–926. [PubMed: 1959135]

Tabata T, Takei Y. Morphogens, their identification and regulation. Development. 2004; 131:703–712. [PubMed: 14757636]

Tautz D, Pfeifle C. A non-radioactive in situ hybridization method for the localization of specific RNAs in *Drosophila* embryos reveals translational control of the segmentation gene hunchback. Chromosoma. 1989; 98:81–85. [PubMed: 2476281]

Teleman A, Strigini M, Cohen S. Shaping morphogen gradients. Cell. 2001; 105:559–562. [PubMed: 11389824]

Ward EJ, Zhou X, Riddiford LM, Berg CA, Ruohola-Baker H. Border of Notch activity establishes a boundary between the two dorsal appendage tube cell types. Dev Biol. 2006 in press.

Wasserman, L. All of Statistics: A Concise Course in Statistical Inference. New York, NY: Springer-Verlag; 2003.

Wasserman JD, Freeman M. An autoregulatory cascade of EGF receptor signaling patterns the *Drosophila* egg. Cell. 1998; 95:355–364. [PubMed: 9814706]

Weisz PB. Diffusion and chemical transformation. Science. 1973; 179:433–440. [PubMed: 4705341]

Wiley HS, Cunningham DD. A steady state model for analyzing the cellular binding, internalization and degradation of polypeptide ligands. Cell. 1981; 25:433–440. [PubMed: 6269748]

Yakoby N, Bristow CA, Gouzman I, Rossi MP, Gogotsi Y, Schupbach T, Shvartsman SY. Systems level questions in *Drosophila* oogenesis. IEE Proc Syst Biol. 2005; 152:276–284.

Zhu AJ, Scott MP. Incredible journey: how do developmental signals travel through tissue? Genes Dev. 2004; 18:2985–2997. [PubMed: 15601817]
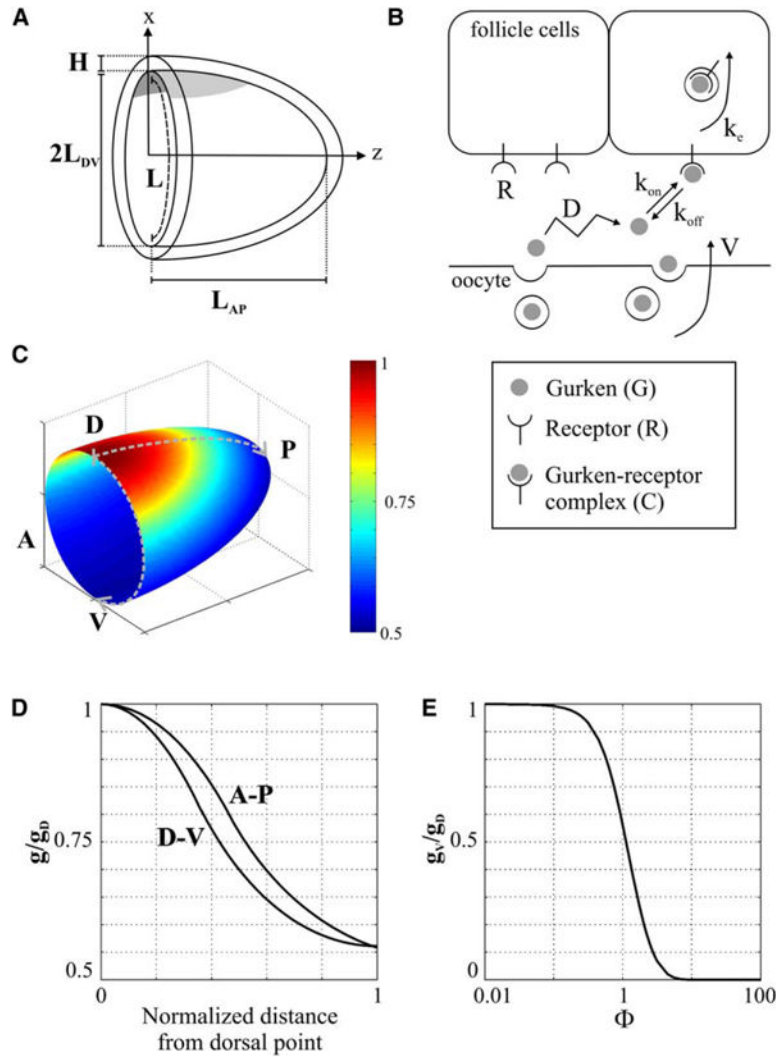
Figure 1. Biophysical Model Gurken Secretion, Diffusion, Binding, and Degradation

(A) The model is formulated in a spheroidal coordinates. H denotes the width of the extracellular gap where ligand transport takes place; L_{DV} and L_{AP} the equatorial and the polar radii of the spheroid modeling the oocyte.

(B) The model includes localized secretion of Gurken from the oocyte (with a constant flux V), ligand transport (with diffusion coefficient D), ligand-receptor binding (with rate constants k_{on} and k_{off}), and ligand-induced endocytosis (with rate constant k_e). The three variables in the model are: G, the concentration of the Gurken molecules; R, the surface density of empty EGF receptors; and C, the surface density of Gurken-EGFR complexes.

(C) The Gurken gradient computed at $\Phi = 1$. D, dorsal; V, ventral; P, posterior; A, anterior.

(D) DV and AP concentration profiles computed for $\Phi = 1$ along the broken lines.

(E) The ratio of Gurken concentrations at the ventralmost and dorsalmost positions at the anterior boundary (denoted by the broken line in [C]), computed as a function of the Thiele modulus. g_D and g_V denote the Gurken concentration at the dorsalmost and ventralmost points, respectively.
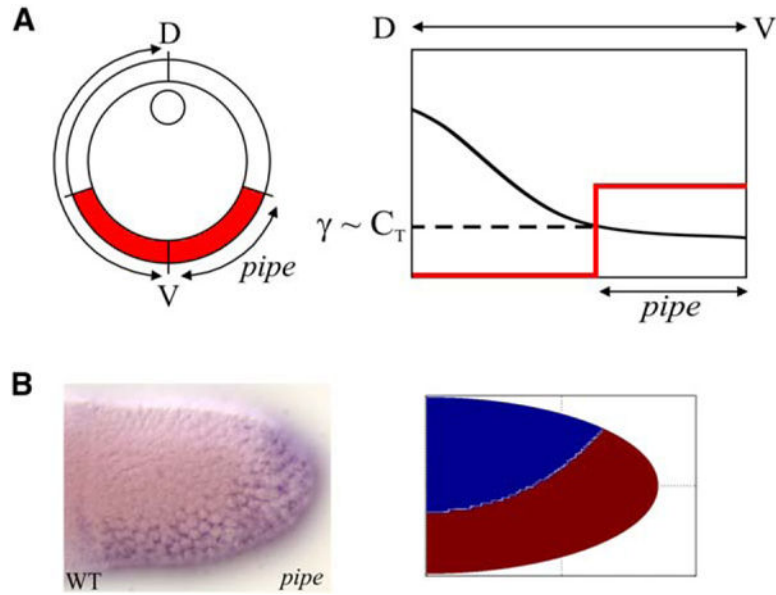
Figure 2. Model of Gurken-Mediated *pipe* Repression

(A) The Gurken-mediated *pipe* repression is modeled as switch-like response (C_T, the concentration of Gurken/EGFR complex at the threshold of *pipe* expression; D, dorsal; V, ventral; L, half circumference of the egg chamber at the anterior boundary).

(B) Comparison between the observed *pipe* staining in wt and the *pipe* domain solved using the procedure described in the text. For an arbitrary value of Thiele modulus (Φ) the threshold parameter γ is computed from the Gurken/EGFR complex concentration at 40% ventral along the anterior cross-section (i.e., the *pipe* domain observed in the wild-type). By using the computed γ at the anterior end, the boundary of *pipe* expression along the AP-direction is determined by tracing the line of equal Gurken/EGFR complex concentration.
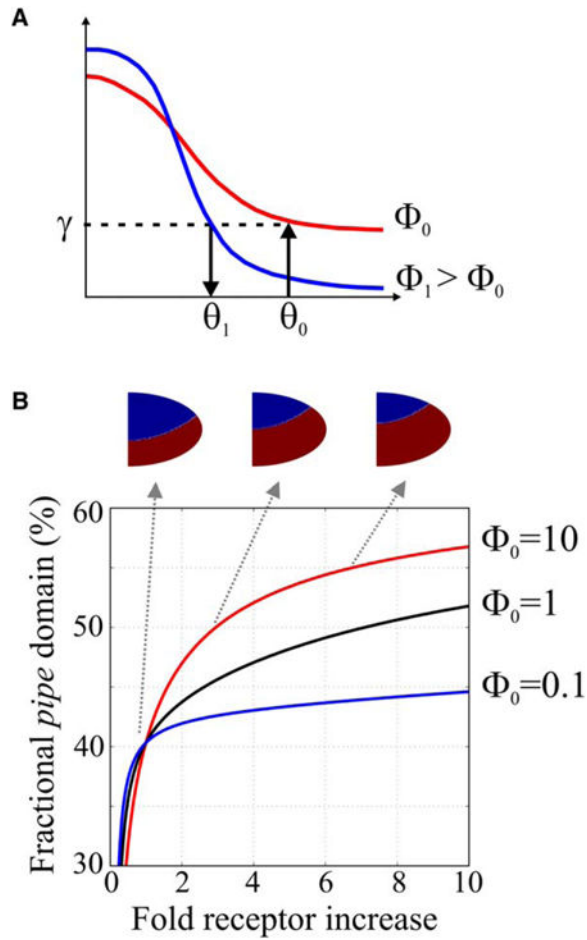
Figure 3. Model Predictions

(A) Graphical illustration of Equation 2: the wild-type location of the boundary of *pipe* expression domain (θ_0) defines the threshold parameter γ for an arbitrarily set starting Thiele modulus (Φ_0). Demanding that γ remain constant as the Thiele modulus changes, it is possible to compute the new domain of *pipe* expression (θ_1) corresponding to the new Thiele modulus (Φ_1). See text for more details.

(B) The Thiele modulus depends on EGFR level in the follicle cells ($\Phi \sim R^{0.5}$). The model predicts that the domain of *pipe* expands/contracts as the receptor level increases/decreases, respectively. Shown are the response curves computed for three different values of the starting Thiele modulus (Φ_0).
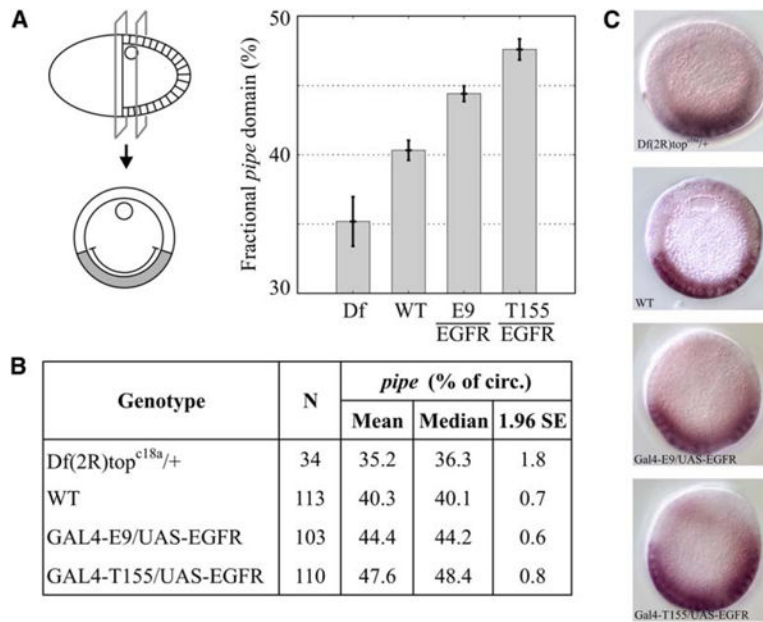
Figure 4. Measurements of the Width of the *pipe* Expression Domain in Genetic Backgrounds with Different Levels of EGFR Expression

Measurements were performed on the cross-sections of egg chambers from late stage 9 to early stage 10B. The differences in the measured *pipe* domains are statistically significant (p < 0.001); error bars in the bar graphs correspond to 1.96SE. No significant correlation was observed between the fractional domain of *pipe* and the size of the egg chambers. The size of the egg chambers is not affected by changes in the receptor level (see Table S1).
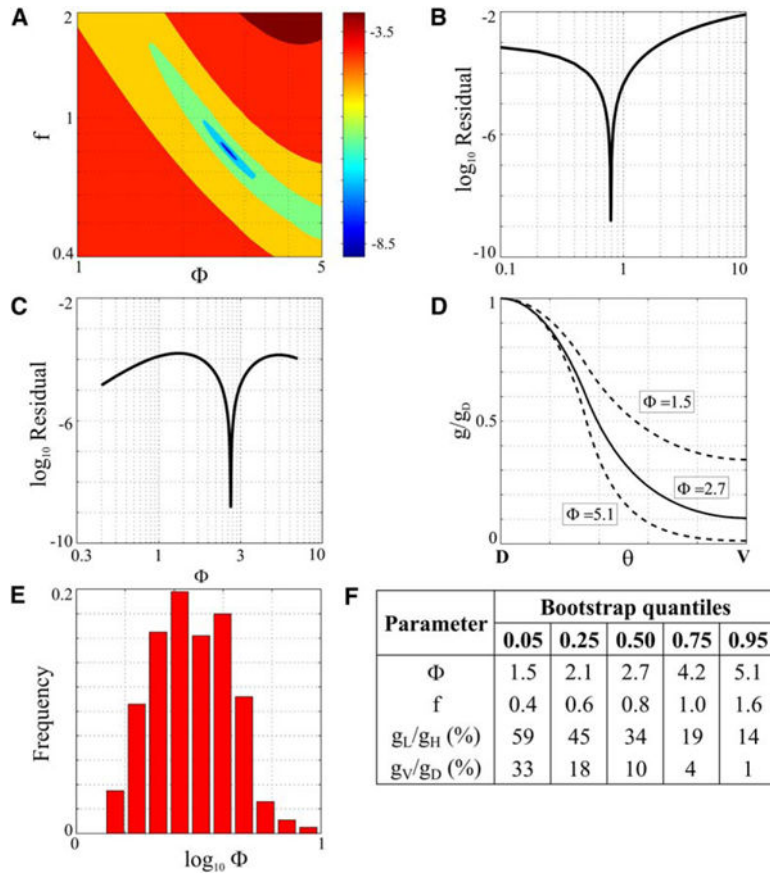
Figure 5. The Thiele Modulus of the Wild-Type Gurken Gradient

(A) A contour plot of the residual from the optimization procedure for finding the estimate of the Thiele modulus. The color bar corresponds to the $\log_{10}$ value of the residual. Based on the medians of the data, the estimate for the Thiele modulus is found to be 2.7.

(B and C) Cross-sections through the minimum of the residual function.

(D) The wild-type Gurken gradient along the anterior circumference, computed with the estimated Thiele modulus. Plotted in the y axis is the Gurken concentration scaled by the maximum concentration at the dorsalmost point. Dotted lines show the profiles computed for Thiele moduli at the boundaries of the 90% confidence interval.

(E) Histogram for the fitted values of the Thiele modulus computed by Bootstrap.

(F) Bootstrap quantiles of the estimated Thiele modulus.
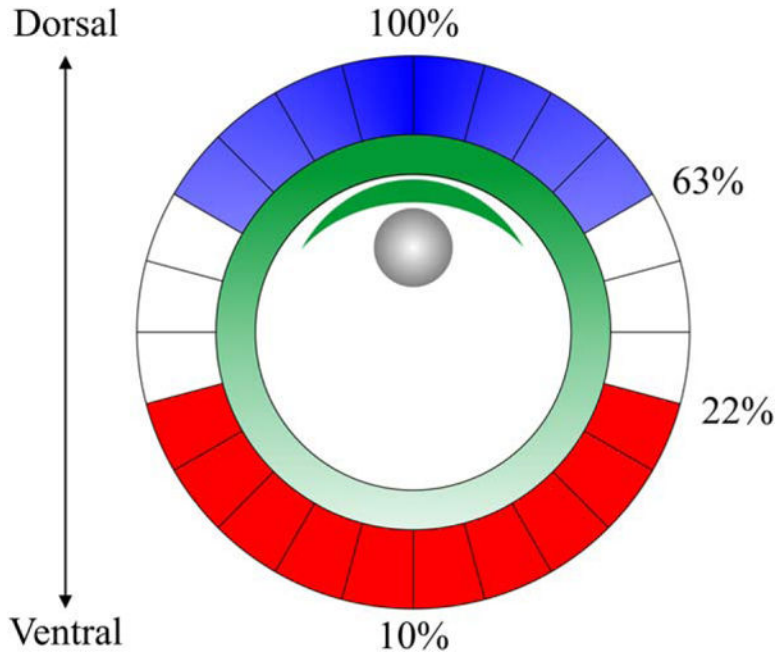
Figure 6. Summary of the Quantitative Analysis of the Gurken Gradient
Gurken is locally secreted from the dorsal anterior cortex of the oocyte and forms a shallow gradient with a Thiele modulus of 2.7 (1.5, 5.1). When normalized to the maximal concentration at the dorsal side, the Gurken gradient drops to 63% (73%, 56%) at one-third dorsal, which coincides roughly with the boundary of the dorsal genes (such as *kekkon* and *sprouty*; blue), 22% (42%, 8%) at the boundary of *pipe* expression (red), and 10% (31%, 1%) at the ventral midline. Numbers in brackets correspond to 90% confidence intervals of the derived estimates.